A Comparative Study of Photoacoustic and Reflectance Methods for Determination of Epidermal Melanin Content

John A. Viator,*† Jason Komadina,‡ Lars O. Svaasand,†§ Guillermo Aguilar,†¶ Bernard Choi,† and J. Stuart Nelson†

*Department of Dermatology, Oregon Health & Science University, Portland, Oregon, USA; †Beckman Laser Institute, University of California, Irvine, California, USA; ‡Harvey Mudd College, Claremont, California, USA; §Norwegian Institute of Technology, Division of Physical Electronics, University of Trondheim, Trondheim, Norway; ¶Department of Mechanical Engineering, University of California, Riverside, California, USA

Although epidermal melanin content has been quantified non-invasively using visible reflectance spectroscopy (VRS), there is currently no way to determine melanin distribution in the epidermis. We have developed a photoacoustic probe that uses a Q-switched, frequency-doubled Nd:YAG (neodymium, yttrium, aluminum, garnet) laser operating at 532 nm to generate acoustic pulses in skin *in vivo*. The probe contained a piezoelectric element that detected photoacoustic waves that were then analyzed for epidermal melanin content using a photoacoustic melanin index (PAMI). Melanin content was compared between results of photoacoustics and VRS. Spectra from human skin were fitted to a model based on diffusion theory that included parameters for epidermal thickness, melanin content, hair color and density, and dermal blood content. Ten human subjects with skin phototypes I–VI were tested using the photoacoustic probe and VRS. A plot of PAMI v. VRS showed a good linear fit with $r^2 = 0.85$. Photoacoustic and VRS measurements are shown for a human subject with vitiligo, indicating that melanin was almost completely absent. We present preliminary modeling for photoacoustic probe design and analysis necessary for depth profiling of epidermal melanin.

Key words: acoustic transducer/optical fiber/optoacoustic/PVDF/skin
J Invest Dermatol 122:1432–1439, 2004

Epidermal melanin, a broadband optical absorber, is found to varying degrees in the human skin, affecting subsurface fluence after laser irradiation using wavelengths less than 1.5 μm (Kollias and Baqer, 1985, 1986, 1987; Svaasand *et al*, 1995, 1996). Any dermatologic laser procedure must consider epidermal melanin content (EMC) in the interpretation of diagnostic information or in dosage estimates for therapy. For example, laser therapy of port wine stains (PWS) must consider EMC in order to optimize laser fluence and cryogen spray cooling parameters (Nelson *et al*, 1995; van Gemert *et al*, 1995; Aguilar *et al*, 2001, 2002). Currently, EMC can be estimated non-invasively with pulsed photothermal radiometry (PPTR) (Jacques *et al*, 1993, 1996; Milner *et al*, 1996; Majaron *et al*, 2002), visible reflectance spectroscopy (VRS) (Kollias and Baqer, 1985, 1986, 1987; Svaasand *et al*, 1995; Zonios *et al*, 2001), and chromameter measurements (Alaluf *et al*, 2002). As PPTR requires analysis using inverse algorithms, determination of EMC is extremely sensitive to input parameters that can lead to inconsistent results. VRS and chromameter measurements show reliable measurements of EMC, although they provide no depth information. Additionally, many VRS systems and chromameters utilize an integrating sphere that averages skin reflectance over a large area (e.g., >1 cm^2), making local estimates of melanin concentration impossible.

Photoacoustic measurements use pulsed laser irradiation to induce rapid thermoelastic expansion in epidermal melanin. Unlike photoacoustic spectroscopy (Rosencwaig, 1980), which uses modulated continuous wave irradiation, photoacoustic generation by thermoelastic expansion can be described conceptually as laser energy quickly absorbed by a small volume such that resultant heating induces rapid expansion that manifests itself as a transient pulse of acoustic energy. Thermoelastic expansion occurs when the condition of stress confinement is achieved, i.e., where optical energy is deposited before propagating away acoustically. This condition is expressed as $t_p < \delta/c_s$, where t_p is the laser pulse duration, δ the absorption depth of laser energy, and c_s is the speed of sound in the medium.

For a laser spot incident on a planar absorber, such as a colored gel sheet in air, the photoacoustic wave is represented by the bipolar waveform shown in Fig 1. This waveform was obtained by irradiating a 185 cm^{-1} absorbing gel with an Nd: YAG laser operating at 532 nm with the acoustic detector underneath the gel sheet. In this transmission mode of acoustic detection, earlier times of the "A" peak represent subsurface regions of photoacoustic generation, whereas the maximum peak occurs at the surface, where laser fluence, and hence photoacoustic pressure, were greatest.

Abbreviations: Γ, Grüneisen coefficient; λ, wavelength; μ_a, optical absorption coefficient; μm, micron; EMC, epidermal melanin content; H0, radiant exposure; Nd, YAG, neodymium, yttrium, aluminum, garnet; nm, nanometer; ns, nanosecond; PAMI, photoacoustic melanin index; PPTR, pulsed photothermal radiometry; PVDF, polyvinylidene fluoride; PWS, port wine stain; $p_0(z)$, pressure at depth, z; VRS, visible reflectance spectroscopy

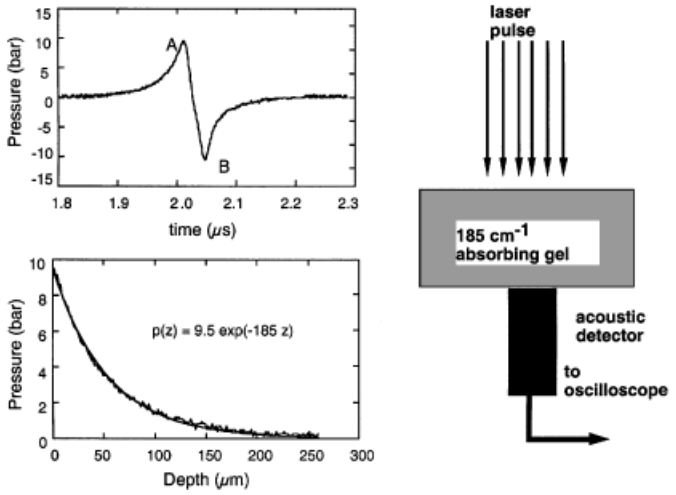

Figure 1
Photoacustic generation in planar gels (Top) An acoustic wave generated by irradiating a 185 per cm gel. The negative wave (*B*) following the positive wave (*A*) is a reflected tensile wave resulting from acoustic mismatch of the gel/air boundary. (Bottom) The absorption information of the acoustic wave is shown here as pressure as a function of gel depth. The apparatus is shown toward the right.

The gel/air interface acts as a free surface, so that half of the acoustic energy travels into the gel (indicated by the "A" peak) and the other half is reflected by the free surface back into the gel (indicated by the "B" peak). Taking the maximum of the "A" peak as the surface and reflecting the waveform to become a function of depth, we obtain the decreasing exponential shown in the lower half of Fig 1. As illustrated in the figure, the amount of light absorbed versus depth decreases exponentially according to Beer's Law. Converting the time axis to depth in tissue by using a sound speed, c_s of 1.5 mm per μs and the relation $z = (t_{peak} - t)c_s$, where t_{peak} is the time of the surface peak and t is time, we obtain a representation as shown in the figure. The exponential curve fit of this acoustic wave contains the absorption coefficient in the exponent,

$$p(z) = 9.5\exp(-185z), \qquad (1)$$

where p(z) is the pressure in bars at depth z in centimeters. This gives an absorption coefficient of 185 per cm from the fit; the measured absorption coefficient from a spectrophotometer was 180 per cm. Thus, the photoacoustic wave shown is related to absorbed optical energy, which corresponds to tissue chromophores. This principle is utilized to measure epidermal melanin in this paper. It must be noted that photoacoustic waves are not necessarily symmetric, as in Fig 1, since the distribution of optical absorbers may not be planar, giving rise to diffractive waves that cause the photoacoustic wave to depart from bipolar symmetry. Analysis of the photoacoustic waves, however, is restricted to the initial pressure pulse, which arrives before the diffractive waves have time to reach the detector.

Photoacoustic spectroscopy has been used by Rosencwaig and Pines (1977a, b), who looked at the absorption spectra of the stratum corneum, studying its hydration and maturation. Photoacoustic spectroscopy, as noted above, however, is distinct from photoacoustic waves arising from thermoelastic expansion. Such methods have been used to determine optical properties of tissue and to perform imaging (Oraevsky *et al*, 1993; Esenaliev *et al*, 1999; Viator *et al*, 1999; Paltauf *et al*, 2002). Viator *et al* (2002) using a photoacoustic probe to distinguish epidermal melanin and PWS layers in human skin *in vivo*. The probe under current study is based on that design.

We have developed a photoacoustic probe that incorporates an optical fiber and piezoelectric detector in a small handpiece to determine EMC in human skin. Laser energy is delivered via the fiber to the skin surface, where it is absorbed by epidermal melanin. The short pulse duration of the laser ensures transduction of optical energy into acoustic waves, analysis of which gives the exact optical energy absorption, which, in turn, is related to the spatial distribution of melanin from which its content can be deduced. Thus, acoustic wave analysis provides the optical energy absorption of a therapeutic laser pulse, giving the clinician valuable information regarding light dosage. We previously tested the probe on layered tissue phantoms made from polyacrylamide gels with optical properties matched to those of normal and PWS human skin (Viator *et al*, 2002).

In this paper, we determined the EMC of ten human subjects using the photoacoustic probe and compared these measurements with VRS. VRS data were fitted to a diffusion theory model, which allowed us to determine EMC. We distinguished the subjects into four classifications based on sun-reactive skin phototypes I–II, III, IV, and V–VI (Fitzpatrick, 1988). A plot of melanin content as determined by photoacoustic v. VRS means showed a strong correlation between the two methods, with a linear fit showing a slope of 0.58 ($r^2 = 0.85$).

This paper marks the initial work using photoacoustic analysis to measure EMC in human skin. Although no attempt has been made to determine absolute EMC, the purpose of this paper is to show a correlation between photoacoustic measurements and VRS, a well-developed method to measure EMC. We also discuss future work to utilize photoacoustics and extend the analysis to perform depth profiling and imaging in human skin.

Results

Photoacoustic signals Four photoacoustic signals representing skin phototypes I-II, III, IV, and V-VI are shown in Fig 2.

Pressure amplitude and total energy, indicated by the area under the waveform, increase with skin phototype. The complicated nature of the waveforms, which depart from the simple form of Fig 1, is due to the irregular distribution of epidermal melanin and the fact that the acoustic waves were integrated over the entire surface of the 200 μm active area of the PVDF.

VRS measurements Four VRS signals representing the same measurements of skin phototypes I-II, III, IV, and V-VI are shown in Fig 3 as solid lines. Model fits are shown as dotted lines.

Increasing melanin content obscures the oxyhemoglobin-induced minima in skin reflectance at 550 and 577 nm.

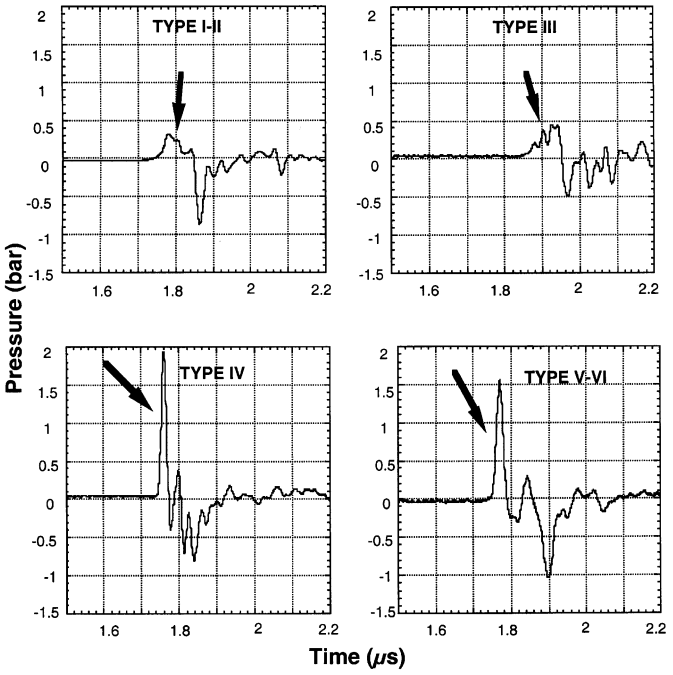

Figure 2
Photoacoustic signals for the four classifications of skin phototypes. EMC is related to the area under the first positive peak, indicated by the arrows.

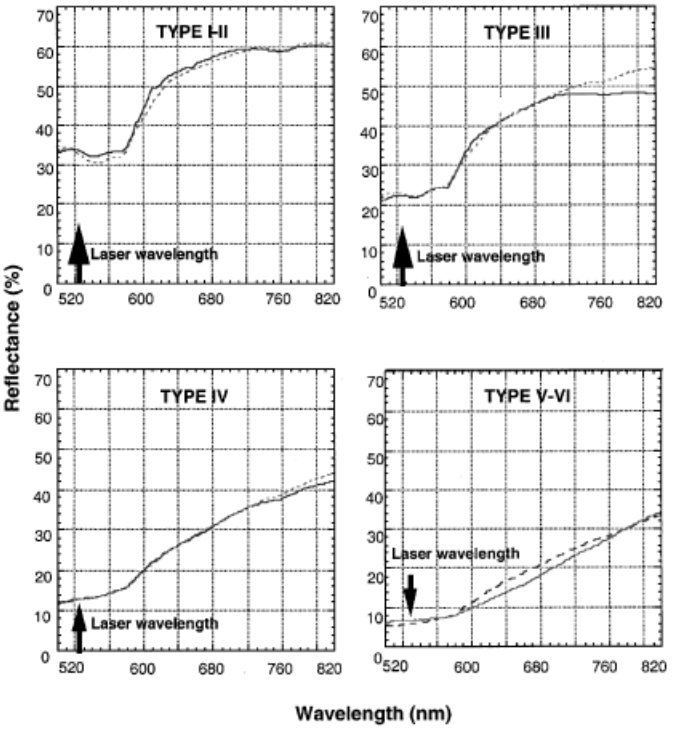

Figure 3
VRS measurements and diffusion model fits for the four classifications of skin phototypes. Spectra are shown as solid lines, and model fits are shown as dotted lines. EMC is inversely related to the slope of the spectra from 585 to 630 nm, where increasing slope indicates decreasing melanin content. Arrows indicate the laser wavelength used in the photoacoustic measurements.

Measurements on a subject with vitiligo Photoacoustic and VRS measurements of a vitiligo site are shown in Fig 4. The photoacoustic amplitude is very low, with a small peak of less than 0.1 bar. The additional structure beyond 1.7 μs is probably due to acoustic diffraction caused by hemoglobin absorption in the dermis. The VRS measurement shows high reflectance, although there may be a small component of melanin in this measurement due to the fact that the input port of the integrating sphere was slightly larger than the vitiligo spot.

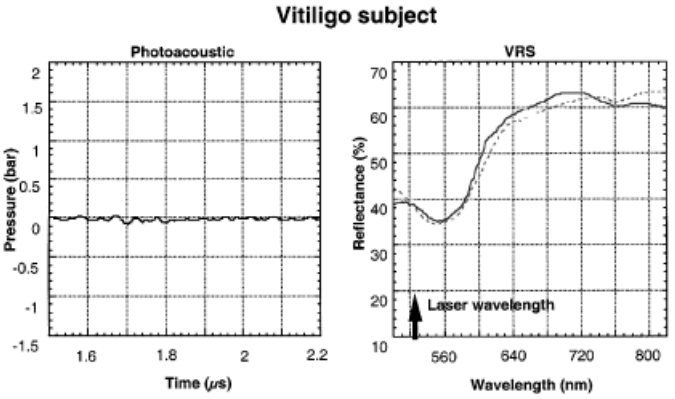

Figure 4
Photoacoustic and VRS measurements of a subject with vitiligo. The small peak at 1.7 μs in the photoacoustic plot indicates minor absorption probably due to deoxygenated hemoglobin, which is evident in the VRS plot.

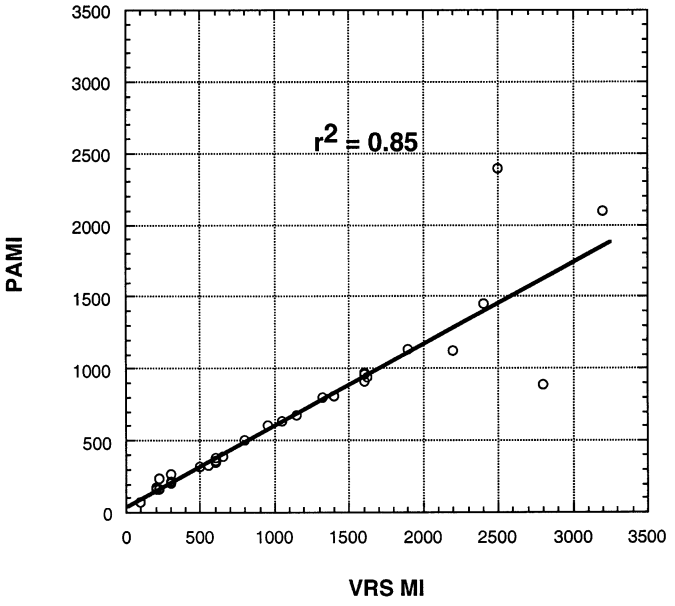

Figure 5
VRS measurements are plotted against PAMI to show the correlation between the two measurement methods ($r^2 = 0.85$). The correlation breaks down for darker skin phototypes, probably due to the small absorption depths.

Comparison of photoacoustic and VRS results The spectroscopic melanin index (VRSMI) was plotted against the PAMI (Fig 5).

A linear fit closely follows the data, expressed as $\text{PAMI} = 0.58 \times \text{VRSMI} + 32$. The correlation was good, with $r^2 = 0.85$. There are 30 data points, as each subject was measured in three locations.

Figure 6 shows the average total melanin index determined by each skin phototype for the photoacoustic

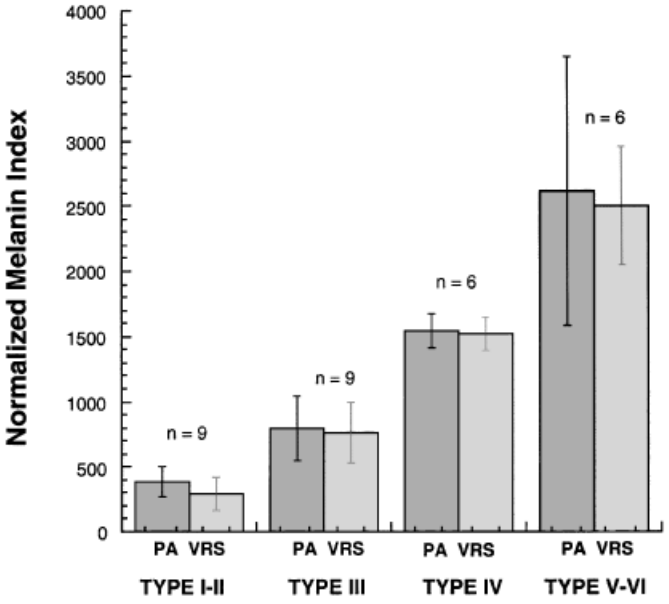

Figure 6
Photoacoustic and VRS measurements of epidermal melanin are shown for the four classifications skin phototypes I–II, III, IV, and V–VI.

method and VRS. As expected, melanin content increases with skin phototype, although large standard deviations exist.

Discussion

Accurate, repeatable measurements of EMC are important for dermatologic laser procedures as well as for diagnosis of pigmented dermatoses. Epidermal melanin is difficult to measure or characterize non-invasively as *in vitro* and *in vivo* measurements can vary greatly due to hydration, chromophore distribution, and other factors can change the mechanisms of light interaction with melanin. Wolbarsht *et al* (1981), hypothesized that the dominant mechanism of light interaction with melanin is not absorption, but scattering, thereby describing the concept of the melanosome as a light trap in which photons are scattered therein and subsequently absorbed. The distribution of epidermal melanin is a dynamic process in which melanocytes in the basal layer transfer melanosomes to keratinocytes, which subsequently degrade the melanin granules as they migrate toward the skin surface (Young, 1997). The distribution of epidermal melanin is unclear, as some studies have shown that melanin does not extend above the deeper layers of the epidermis in skin phototypes I–II, whereas in skin phototypes V–VI it extends to the surface corneocytes. Lu *et al* (1996), however, have shown that even in skin phototype II, melanin can be found in the corneocytes.

Fortunately, for the clinician performing dermatologic laser procedures, measurement of EMC does not require in-depth knowledge of melanosome production and transfer. The photoacoustic wave generated in skin gives the exact distribution of optical absorption in the epidermis immediately after laser irradiation, from which a proper light dosage can be determined. If the therapeutic pulse is at a different wavelength from the diagnostic (photoacoustic) pulse, light dosage can be calculated knowing the absorption spectrum of melanin. Alternatively, the photoacoustic laser can be tuned, using an optical parametric oscillator, to match the therapeutic laser wavelength. This procedure could also be performed using VRS, although the photoacoustic procedure has the potential to provide additional information about the depth profile of epidermal melanin. The use of multiple wavelengths can also be used to target specific chromophores, so that different tissue structures may be differentiated. An example would be to use 760 nm light to differentiate oxygenated from deoxygenated hemoglobin, due to the absorption peak in the latter spectrum.

VRS measurements VRS measurements were obtained for comparison with photoacoustic experiments. Previous studies have used Monte Carlo models (Meglinski *et al*, 2002) and diffusion theory (Zonios *et al*, 1999, 2001). A model based on diffusion theory in two layers was used here; one layer with optical properties matched to epidermis, and the second with optical properties matched to the dermis. Even with the relatively simple parameters discussed in Materials and Methods, we obtained good fits for all spectra taken. EMC was estimated by focusing on matching the slope of the spectrum from 585 to 630 nm, a region where melanin absorption dominates, thus avoiding high hemoglobin and water absorption. Minor departures from good fits can be seen in Fig 3 in the skin phototype III measurements. The divergence between model and experimental spectra occurs after 700 nm and did not affect the estimated EMC. This divergence may have been due to inexact estimation of water absorption, which is of importance in this region.

Photoacoustic measurements The calculation of PAMI was simple and can be conceptually described as the area beneath the photoacoustic wave and corresponds to the total optical energy absorbed by epidermal melanin.

As long as epidermal thickness is such that it permits at least 10% transmission, this approximation scheme is valid. If the thickness is much greater, then the PAMI would indicate a lower limit for melanin concentration. This only occurs for skin phototypes V–VI, however, as the absorption coefficient for a 100 μm thick epidermis would have to be greater than 200 per cm, meaning that the melanin volume fraction would have to be greater than 30% over the entire epidermis. This analysis assumes a melanosome absorption coefficient of about 550 cm^{-1} at 532 nm, which follows from,

$$\mu_s = 1.70 \times 10^{12} \lambda^{-3.48}, \qquad (2)$$

which is an approximation from Jacques *et al* (1996), with λ in nm.

Durations of the photoacoustic waves give some indication of the epidermal melanin depth profiles. A longer duration implies that melanin is distributed throughout the epidermis, whereas a short duration indicates that melanin is probably confined to the basal layer. A strict depth profile cannot be assumed from this data, however, due to the fact that the epidermal–dermal junction is non-planar and due to limitations of the current photoacoustic probe design.

Laser fluence in this study ranged up to 0.35 J per cm^2, which is within the range of 0.1–1 J per cm^2 previously

reported to rupture epidermal melanosomes at this wavelength and pulse duration (Anderson *et al*, 1989; Jacques and MacAuliffe, 1991). Laser-induced melanosome rupture is considered to be a cavitation process, which does not produce simple thermoelastic acoustic waves in accordance with our model. Although gross immediate skin whitening due to melanosome rupture was not observed, some melanosome rupture may have occurred at the higher fluences used in our study. Ideally, fluences for photoacoustic determination of EMC at 532 nm should be below about 0.1 J per cm^2.

Vitiligo subject VRS showed a low EMC at the limit of the model' detection ability. The resultant photoacoustic wave showed a small peak of less than 0.1 bar, about one order of magnitude less than the measurement for a typical Phototype III subject. The detection port on the integrating sphere of the VRS system was 25.4 mm in diameter, which was slightly larger than the actual vitiligo site studied, thus the total reflectance may have been higher. VRS showed a strong contribution from deoxygenated hemoglobin, which we have found in some or our measurements of elderly patients. This may be due to age-related circulatory problems, although our data are not conclusive in this regard.

Comparison of photoacoustic and VRS measurements The correlation for PAMI and VRS was good, and limiting measurements to skin phototypes I–IV would have yielded an even better fit, as skin phototypes V–VI showed greater divergence. This divergence may have been due to the uncertainty in hemoglobin reflectance, as the actual value was masked by the intervening EMC. Future studies may include methods to decrease the hemoglobin contribution, perhaps by inducing vasoconstriction, although the current protocol did not allow for such procedures. It is clear that this shortcoming must be investigated, as measurement of highly pigmented skin is of great clinical interest.

Differences in VRS and photoacoustics modalities must be mentioned. The active area of the photoacoustic method is approximately 200 μm, making pinpoint measurements possible, although local variations due to the presence of hair follicles could greatly overestimate EMC. Thus it is prudent to avoid hair during photoacoustic measurements. With VRS, the EMC is approximated from an average of a 1 in diameter area, smoothing out such local variations, but making pinpoint measurements impossible. We took measures to ensure that artifacts due to abnormal pigmentation and hair follicles were avoided.

Future work As shown, epidermal melanin depth profiles can in theory be derived from photoacoustic signals. This was not possible, however, with the single detector apparatus of this pilot study. Melanin concentration is generally higher in the epidermal basal cell layer, which is not flat as it follows the contours of dermal papillae. The difficulty of determining melanin depth profile with the current probe was estimated by computer simulation according to Equation (3) (the simulation is fully described in Paltauf *et al*, 2002). The detector was simulated to be 1 mm above the surface of a 0.1 mm thick epidermis, overlying a thick, non-absorbing dermis. The epidermal absorption coefficient was set to be 25 per cm, in either a uniform layer or a sinusoidally varying pattern to mimic the typical undulations of epidermal thickness (rete pattern). In this model, epidermal undulations reduced peak amplitude and increased decay time from the simulated acoustic detector, in a manner indistinguishable from a planar epidermis with less absorption. Acoustic waves from complex melanin distributions are superimposed on a single detector; our simulation model suggests that using multiple acoustic detectors may in the future allow us to map actual melanin distributions *in vivo*.

Materials and Methods

Photoacoustic apparatus Figure 7 shows the apparatus for photoacoustic measurements that consisted of a laser, optical fiber, probe, and detection electronics.

The laser was a Q-switched, frequency-doubled Nd:YAG (Quantel Brilliant, Big Sky Laser, Bozeman, Montana) operating at 532 nm with a pulse duration of 4 ns. The laser output was coupled into a 1000 μm diameter quartz optical fiber that terminated in a small, cylindrical acrylic handpiece, measuring 16 mm in diameter and 22 mm in length. The optical fiber was directed to a 1.5 mm spot at the bottom of the probe, which was placed onto the skin surface for measurements. Laser energy ranged from 3 to 6 mJ per pulse in all experiments, although pulse energy was determined to 5% accuracy for each measurement. Radiant exposures were approximately 0.15–0.35 J per cm^2. A piezoelectric element made from polyvinylidene fluoride (PVDF), which was recessed 3 mm into the probe housing, detected any photoacoustic waves generated by laser light and created an acoustic delay of approximately 2 μs. Water was used to couple the sensor and skin surface acoustically. The piezoelectric element was attached to a rigid coaxial cable that was connected to an instrumentation amplifier with a gain of 125 (SR445, Stanford Research Systems, Sunnyvale, California). The amplified signal was sent to an oscilloscope (TDS 3014, Tektronix, Wilsonville, Oregon) with a bandwidth of 100 MHz sampled at 1.25 gigasamples per second and was triggered by a photodiode (DET-210, Thorlabs, Newton, New Jersey) that monitored laser output. The waveforms were averages of 32 pulses. Stable waveforms during averaging suggested repeatability of acoustic generation in melanin. The laser pulse constituted $t = 0$. Photoacoustic waves were analyzed on a computer (G4 Powerbook, Apple Computer, Cupertino, California) using Mathematica 4.1 (Wolfram Research, Urbana, Illinois).

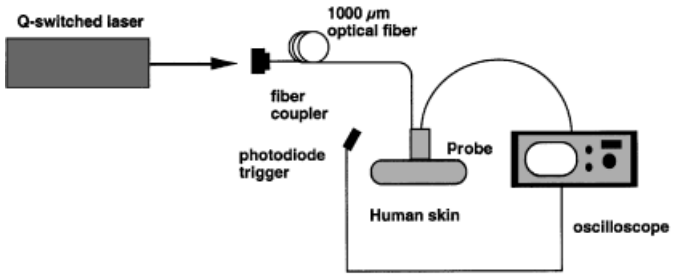

Figure 7
Apparatus for photoacoustic depth determination of melanin content. The frequency-doubled 532 nm Nd:YAG laser had a pulse duration of 4 ns. Laser light was delivered to the probe via 1000 diameter optical fiber. A PVDF element within the probe detected photoacoustic waves.

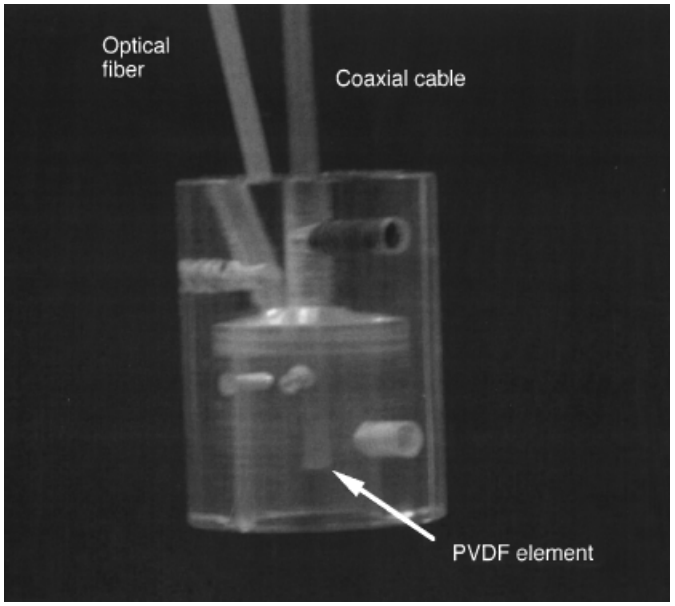

Figure 8
The photoacoustic probe is shown here. The optical fiber delivered 532 nm laser light with a pulse duration of 4 ns. Acoustic detection was obtained by a PVDF element within the probe cavity. The PVDF was recessed approximately 3 mm from the bottom of the probe, thus initial photoacoustic waves were delayed approximately 2 μs from the laser pulse.

The probe is shown in Fig 8.

The PVDF element can be seen in the inner chamber, which was filled with water after the probe was placed in contact with the skin. There was no floor on the chamber in order to prevent an acoustic interface between the tissue and sensor. Thus, when placed in contact with skin, some tissue would bulge into the chamber, decreasing the distance from the skin surface to the sensor. This had the effect of changing the timing of the photoacoustic signal, making an absolute surface position measurement impossible. A glass window could have been added, but this would have given rise to acoustic reflections. As surface position was not important in this study, the probe design remained without the window.

Photoacoustic analysis Photoacoustic waves were induced by irradiating with a stress-confined laser pulse of 4 ns duration. Photoacoustic generation was achieved by the mechanism of thermoelastic expansion caused by rapid tissue heating. For laser irradiation on a planar absorber (a good approximation of the lateral distribution of melanin in skin), such thermoelastic expansion results in an acoustic wave described by,

$$p_0(z) = \tfrac{1}{2}\mu_a \Gamma H_0 \exp(-\mu_a z), \quad (3)$$

where $p_0(z)$ is the initial pressure at depth z, μ_a is the chromophore absorption coefficient, and Γ is the unitless Grüneisen coefficient, which describes the fraction of optical energy translated into energy for thermoelastic expansion. The value $\Gamma = 0.12$ used in this paper was for tissue at room temperature (Oraevsky *et al*, 1993). H_0 is the incident laser radiant exposure. The factor of $1/2$ is due to the approximate planar geometry of human skin, indicating that half of the acoustic energy travels upward, toward the skin surface, with the other half traveling away. The upward component is what was measured from the photoacoustic wave induced in epidermal melanin.

EMC was deduced by analysis of total acoustic energy detected. Since laser spot size (area) was constant, epidermal scattering was assumed to be consistent between human subjects, and light propagation into tissue was only about 100 μm; the total acoustic energy would be directly related to melanin content. Acoustic pressure is proportional to energy per unit volume, often expressed as J per cm3. Since the spot size is constant, the integral of pressure over depth yields the total absorbed energy and can be expressed as

$$E_t \propto \int_0 p_0(z)dz, \quad (4)$$

where E_t is the total absorbed energy and $p_0(z)$ is the initial pressure as a function of depth, z, from Equation (3). The integral gives a quantity that is expressed in terms of J/cm^2, so the total energy detected is related to this quantity by the detector active area. Thus, this integral is proportional to EMC and, after normalizing by total pulse energy, can be defined as a preliminary photoacoustic melanin index (pPAMI). This index is still dependent on acoustic detector active area, so scaling by active area gives a device-independent PAMI. Scaling of the active area was achieved by taking the ratio of active area to laser spot size; hence, PAMI is dimensionless.

$$\mathrm{PAMI} = \frac{A_t \int_0 p_0(z)dz}{A_s E_t}. \quad (5)$$

PAMI was computed for all photoacoustic measurements taken. Blood content within dermal papillae was neglected in this analysis. Although blood contributed to the initial peak of the photoacoustic signal, it was assumed to be constant between subjects, as well as being a small contribution to the overall photoacoustic pressure. This assumption is supported by the small amplitude pressure in the vitiligo subject, in which the dominant chromophore is blood.

VRS apparatus The apparatus for performing VRS measurements consisted of a spectrometer, white light source, integrating sphere, and computer (Fig 9).

The spectrometer (HP 8452A, Hewlett-Packard, Palo Alto, California) was optimized for detection of 190–820 nm light, although our analysis was confined to 500–820 nm with a wavelength accuracy of 2 nm. The light source was a tungsten halogen lamp within the integrating sphere (RSA-HP-84, Labsphere, North Sutton, New Hampshire) and was coupled to the

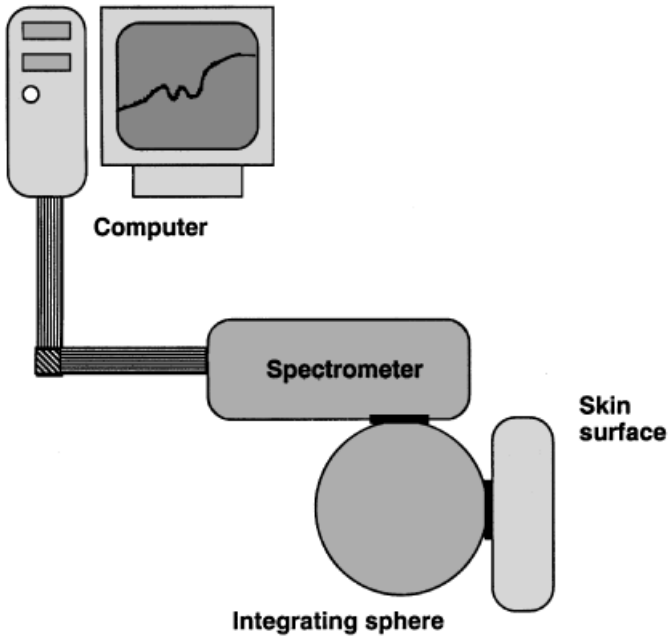

Figure 9
Apparatus for VRS measurement of EMC. The spectrometer data were taken from 500 to 820 nm. The integrating sphere port was 25.4 mm in diameter. All measurements were normalized to a 99% reflectance standard.

Table I. Parameters varied during the fit of the VRS data

Hematocrit	HbO_2	Melanin	Water (epi)	Water (derm)	Blood (epi)	Blood (derm)	δ_{epi}	δ_{derm}
0.41–0.45	0.65–0.85	2.0–28.0	0.60	0.70–0.80	0.001	0.015–0.04	200–500	200–500

Deoxygenated hemoglobin was 1-HbO_2. Melanin and epidermal and dermal scattering (δ_{epi} and δ_{derm}, respectively) are given per cm. Other values are in volume fraction.

spectrometer controlled by a Pentium computer. The skin surface of human subjects was positioned at the 25.4 mm diameter port of the integrating sphere and sampled with an integration time of 500 ms. UV-Visible ChemStation software (Hewlett-Packard) was used as an interface to the spectrometer. A 99% diffuse reflectance standard (WS-1, Ocean Optics, Dunedin, Florida) was used to calibrate the spectrometer.

VRS analysis VRS measurements resulted in spectra from 500 to 820 nm as percent diffuse reflectance. The spectra were fitted to a diffusion model based on Svaasand *et al* (1995), which showed the entire development of the diffusion model and treated the subject in detail in an appendix. The two-layer model was developed consisting of a thin 100 μm epidermis over a semi-infinite dermis. Absorption in the epidermis was primarily due to melanin and a small fraction of blood in the vascular dermal papillae extending into the most superficial 100 μm of human skin. Dermal absorption was primarily due to oxygenated and deoxygenated hemoglobin. Hematocrit and relative blood oxygenation were variable, normally set at 0.41% and 70%, respectively. Both layers had wavelength-dependent scattering, following λ^{-1} where λ is the wavelength, and a small background component of absorption. Additionally, water was included as an absorber in the infrared, with epidermal and dermal water contents set at 60% and 80%, respectively. Absorption and scattering were expressed as analytic functions incorporated into a computational model using Maple 6.01 (Waterloo Maple, Ontario, Canada). Absorption by hair follicles was also included in the model, with parameters including hair color and density, melanin content, and shaft thickness. In the experiments, hair was avoided in VRS measurements and thus the hair parameters in the model were set to zero. The parameters that were varied are shown in Table I, as well as the range in which they were varied. All quantities in the table are volume fraction, except for melanin and epidermal and dermal scattering, which were given per cm.

Fitting was accomplished primarily by varying melanin and blood concentrations in the model, although relative blood oxygenation and background absorbance levels were also varied to improve the fit. Melanin content was optimized by matching the slope of the spectrum from 585 to 630 nm, where the effect of melanin on reflectance would be most evident. Although oxygenated and deoxygenated hemoglobin absorption are well over 100 per cm at 585 nm, they drop off to less than 10 per cm at 630 nm. Additionally, the spectra are similar in this range, with deoxygenated hemoglobin far exceeding oxygenated hemoglobin absorption above 630 nm. Therefore, this range was chosen to derive the melanin content. VRS Melanin Index (VRS MI) is the absorption coefficient of epidermal melanin at 690 nm used in the diffusion theory model fit.

Human subjects We tested ten healthy human subjects using the photoacoustic probe and VRS. All institutional rules governing clinical investigation of human subjects were strictly followed. We conformed to the Helsinki Declaration with respect to human subjects in biomedical research.

Three sites were studied on each subject: left dorsal hand, left inner forearm, and central forehead. Care was taken to relocate the same sites on each subject. The numbers of subjects with respect to sun reactive skin phototype are as follows: Phototypes I–II—3; Phototype III—3; Phototype IV—2; and Phototypes V–VI—2. Additionally, an elderly female subject with vitiligo was studied. The vitiligo was on the subject's hands and appeared as irregularly shaped 3–20 mm diameter spots.

This work was supported by research grants from the National Institutes of Health (AR48453, GM62177, AR-47551, HD42057), US Air Force Office of Scientific Research (F49620-00-1-0371), the American Society for Laser Medicine and Surgery Member Research Grant, and the Arnold and Mabel Beckman Fellows Program. Dr Viator was supported by NIH F32GM66693-01.

DOI: 10.1111/j.0022-202X.2004.22610.x

Manuscript received February 20, 2003; revised December 16, 2003; accepted for publication January 6, 2004

Address correspondence to: John A. Viator, Department of Dermatology, OP06, Oregon Health & Science University, 3181 SW Sam Jackson Park Road, Portland, OR 97239, USA. Email: viatorj@ohsu.edu

References

Aguilar G, Diaz S, Lavernia EJ, Nelson JS: Cryogen spray cooling efficiency: Improvement of port wine stain laser therapy through multiple-intermittent cryogen spurts and laser pulses. Lasers Surg Med 31:27–35, 2002

Aguilar G, Majaron B, Viator JA, *et al*: Influence of spraying distance and post-cooling on cryogen spray cooling for dermatologic laser surgery. Proc SPIE 4244:82–92, 2001

Alaluf S, Atkins D, Barrett K, Blount M, Carter N, Heath A: The impact of epidermal melanin on objective measurements of human skin colour. Pigment Cell Res 15:119–126, 2002

Anderson RR, Margolis RJ, Watenabe S, Flotte T, Hruza GJ, Dover JS: Selective photothermolysis of cutaneous pigmentation by Q-switched Nd: YAG laser pulses at 1064, 532, and 355 nm. J Invest Dermatol 93:28–32, 1989

Esenaliev RO, Karabutov AA, Oraevsky AA: Sensitivity of laser opto-acoustic imaging in detection of small deeply embedded tumors. J Select Topics Quant Electron 5:981–988, 1999

Fitzpatrick TB: The validity and practicality of sun-reactive skin types I through VI. Arch Dermatol 124:869–871, 1988

Jacques SL, Glickman RD, Schwartz JA: Internal absorption coefficient and threshold for pulsed laser disruption of melanosomes isolated from retinal pigment epithelium. Proc SPIE 2681:468–477, 1996

Jacques SL, McAuliffe DJ: The melanosome: Threshold temperature for explosive vaporization and internal absorption coefficient during pulsed laser irradiation. Photochem Photobiol 53:769–775, 1991

Jacques SL, Nelson JS, Wright WH, Milner TE: Pulsed photothermal radiometry of port-wine-stain lesions. Appl Optics 32:2439–2446, 1993

Kollias N, Baqer A: Spectroscopic characteristics of human melanin *in vivo*. J Invest Dermatol 85:38–42, 1985

Kollias N, Baqer A: On the assessment of melanin in human skin *in vivo*. Photochem Photobiol 43:49–54, 1986

Kollias N, Baqer AH: Absorption mechanisms of human melanin in the visible, 400–720 nm. J Invest Dermatol 89:384–388, 1987

Lu H, Edwards C, Gaskell S, Pearse A, Marks R: Melanin content and distribution in the surface corneocytes with skin phototypes. Brit J Dermatol 135:263–267, 1996

Majaron B, Verkruysse W, Tanenbaum BS, Milner TE, Nelson JS: Spectral variation of the infrared absorption coefficient in pulsed photothermal profiling of biological samples. Phys Med Biol 47:1929–1946, 2002

Meglinski IV, Matcher SJ: Quantitative assessment of skin layers absorption and skin reflectance spectra simulations in the visible and near-infrared spectral regions. Physiol Meas 23:741–753, 2002

Milner TE, Smithies DJ, Goodman DM, Lau A, Nelson JS: Depth determination of chromophores in human skin by pulsed photothermal radiometry. Appl Optics 35:3379–3385, 1996

Nelson JS, Milner TE, Anvari B, Tanenbaum BS, Kimel S, Svaasand LO: Dynamic epidermal cooling during pulsed laser treatment of port wine stain—a new methodology with preliminary clinical evaluation. Arch Dermatol 131:695–700, 1995

Oraevsky AA, Jacques SL, Tittel FK: Determination of tissue optical properties by piezoelectric detection of laser-induced stress waves. Proc SPIE 1882:86–101, 1993

Paltauf G, Viator JA, Prahl SA, Jacques SL: Iterative reconstruction algorithm for optoacoustic imaging. J Acoust Soc Am 112:1536–1544, 2002

Rosencwaig A: Photoacoustics and photoacoustic spectroscopy. New York: John Wiley & Sons, 1980

Rosencwaig A, Pines E: A photoacoustic study of newborn rat stratum corneum. Biochim Biophys Acta 493:10–23, 1977

Rosencwaig A, Pines E: Stratum corneum studies with photoacoustic spectroscopy. J Invest Dermatol 69:296–298, 1977

Svaasand LO, Fiskerstrand EJ, Kopstad G, Norvang LT, Svaasand EK, Nelson JS, Berns MW: Therapeutic response during pulsed laser treatment of port-wine stains: Dependence on vessel diameter and depth in dermis. Laser Med Sci 10:235–243, 1996

Svaasand LO, Norvang LT, Fiskerstrand EJ, Stopps EKS, Berns MW, Nelson JS: Tissue parameters determining the visual appearance of normal skin and port-wine stains. Lasers Med Sci 10:55–65, 1995

van Gemert MJC, Welch AJ, Pickering JW, Tan OT: Optical–Thermal Response of Laser-Irradiated Tissue. New York: Plenum Press, 1995

Viator JA, Au G, Paltauf G, *et al*: Clinical testing of a photoacoustic probe for port wine stain depth determination. Lasers Surg Med 30:141–148, 2002

Viator JA, Jacques SL, Prahl SA: Depth profiling of absorbing soft materials using photoacoustic methods. J Select Topics Quant Electron 5:989–996, 1999

Wolbarsht ML, Walsh AW, George G: Melanin, a unique biological absorber. Appl Optics 20:2184–2186, 1981

Young AR: Chromophores in human skin. Phys Med Biol 42:789–802, 1997

Zonios G, Bykowski J, Kollias N: Skin melanin, hemoglobin, and light scattering properties can be quantitatively assessed *in vivo* using diffuse reflectance spectroscopy. J Invest Dermatol 117:1452–1457, 2001

Zonios G, Perelman LT, Backkman V, Manoharan R, Fitzmaurice M, Dam JV, Feld MS: Diffuse reflectance spectroscopy of human adenomatous colon polyps *in vivo*. Appl Optics 38:6628–6637, 1999